

Eurographics Workshop on 3D Object Retrieval (2011), pp. 1–5
H. Laga, T. Schreck, A. Ferreira, A. Godil, and I. Pratikakis (Editors)

Selecting 3D Curves on the Nasal Surface using AdaBoost for Person Authentication

L. Ballihi^{†1,2} and B. Ben Amor^{1,3} and M. Daoudi^{1,3} and A. Srivastava⁴ and D. Aboutajdine²

¹Laboratoire d'Informatique Fondamentale de Lille (UMR 8022), Villeneuve d'Ascq Cedex France.

²LRIT, Unité Associée au CNRST (URAC 29), Faculté des Sciences, Université Mohammed V - Agdal, Rabat, Maroc.

³Institut TELECOM ; TELECOM Lille 1, Villeneuve d'Ascq Cedex France.

⁴Department of Statistics, Florida State University, Tallahassee, FL 32306, USA.

Abstract

The main contribution of this paper is the use of an AdaBoost-based learning algorithm which builds a strong classifier from a set of weak classifiers associated with level curves in the nasal region of 3D faces. Its main application is person authentication. The basic idea is to represent nasal surfaces using indexed collections of level curves, and to compare shapes of noses by comparing the shape of their corresponding curves. AdaBoost considers each curve as a weak classifier and iteratively selects relevant curves to increase the authentication accuracy. We demonstrate these ideas on a subset taken from FRGC v2 (Face Recognition Grand Challenge) database. The proposed approach increases authentication performances relative to a simple fusion of scores from all curves.

Categories and Subject Descriptors (according to ACM CCS):

I.2.10 [Computing Methodologies]: ARTIFICIAL INTELLIGENCE/ Vision and Scene Understanding—Shape

1. Introduction

In order to meet the needs of security, a growing international concern, biometrics is presented as a potentially powerful solution. Biometrics aim to use behavioral and/or physiological characteristics of people to recognize them or to verify their identities. In particular, fingerprint and iris-based systems have shown good performances. However they require cooperation of users who may find them intrusive. Since face recognition is contactless and less restrictive, it emerges as a more attractive and natural biometric for security applications. In the last few years, face recognition using the 3D shape of the face has emerged as a major research trend due to its theoretical robustness to lighting condition and pose variations. However, the problem remains open on the issue of robustness of these approaches to facial expressions [AAC06].

To deal with facial expression variations, Bronstein et al. [BBK07] use a geodesic distance function that are invariant to rigid motions and also to facial expressions to some

extent. Similarly in [MMS07], Mpiperis et al. modify their initial geodesic polar parameterization by disconnecting the lips. The second alternative is to restrict the study to a part of the face that remains stable during facial expressions such as ear [YB07, CB07] and nose [CBF06, DASD09]. Blanz et al. [BV03] proposed a new approach based on a morphable model of 3D faces that captures the class-specific properties of faces. Faltmier et al. [FBF08] propose to match independently a committee of regions and then combine the results.

Many of the early methods on 3-D face recognition based on curves, Samir et al. [SSDK09] used the level curves of the geodesic distance function that resulted in 3D curves. They used a non-elastic metric and a path-straightening method to compute geodesics between these curves. Here also, the matching was not studied and the correspondence of curves and points across faces was simply linear. The question is how to choose the curves which can give best results? Frank et al. [tHV09] proposed a 3D face matching framework that allows profile and contour based face matching.

In this work, we focus on the geometric shape analysis of the nose. The basic idea is to approximate a nasal surface by a finite set of geodesic level curves. Using the Riemannian

[†] Chairman Eurographics Publications Board

geometry we define geodesic paths between nasal curves, and elastic distances between them. To compare any two nasal surfaces, we try to combine similarity scores produced by each pair of corresponding curves. We use AdaBoost algorithm to learn a final classifier which identifies and then combines the most relevant curves.

2. Riemannian analysis of nasal surfaces

In the last few years, many approaches have been developed to analyze the shapes of 2D curves. We can cite approaches based on Fourier descriptors, moments or the median axis. More recent works in this area consider a formal definition of shape spaces as a Riemannian manifold of infinite dimension on which they can use the classic tools for statistical analysis. Klassen et al. [KSMJ04] in the case of 2D curves show the efficiency of this approach. Joshi et al. [JKSJ07] have recently proposed a generalization of this work to the case of curves defined in \mathbb{R}^n . We will adopt this work to our problem since our 3D curves are defined in \mathbb{R}^3 .

2.1. Curves analysis in \mathbb{R}^3

We start by considering a closed curve β in \mathbb{R}^3 . Since it is a closed curve, it is natural to parametrize it using $\beta: \mathbb{S}^1 \rightarrow \mathbb{R}^3$. Note that the parameterization is not assumed to be arc-length; we allow a larger class of parameterizations for improved analysis. To analyze the shape of β , we shall represent it mathematically using a square-root velocity function (SRVF), denoted by $q(t)$, according to:

$$q(t) \doteq \frac{\dot{\beta}(t)}{\sqrt{\|\dot{\beta}(t)\|}} \quad (1)$$

Where $\|\cdot\|$ is the Euclidean norm and $q(t)$ is a special function that captures the shape of β and is particularly convenient for shape analysis, as we describe next. The conventional metric for comparing the elastic shape of the curves becomes an \mathbb{L}^2 metric under the representation [JKSJ07, SKJJ10]. Similar ideas were presented by Younes [You98]. We define the set of closed curves in \mathbb{R}^3 by:

$$C = \{q: \mathbb{S}^1 \rightarrow \mathbb{R}^3 \mid \int_{\mathbb{S}^1} q(t) \|q(t)\| dt = 0\} \subset \mathbb{L}^2(\mathbb{S}^1, \mathbb{R}^3) \quad (2)$$

where $\mathbb{L}^2(\mathbb{S}^1, \mathbb{R}^3)$ denotes the set of all integrable functions from \mathbb{S}^1 to \mathbb{R}^3 . The quantity $\int_{\mathbb{S}^1} q(t) \|q(t)\| dt$ is the total displacement in \mathbb{R}^3 while moving from the origin of the curve until the end. When it is zero, the curve is closed. Thus, the set C represents the set of all closed curves in \mathbb{R}^3 . It is called a pre-shape space since curves with same shapes but different orientations and re-parameterizations can be represented by different elements of C . To define a shape, its representation should be independent of its rotations and reparameterization. This is obtained mathematically by a removing the rotation group $SO(3)$ and the reparameterization group Γ

from C . As described in [JKSJ07, SKJJ10], we define the orbits of the rotation group $SO(3)$ and the re-parameterization group Γ as equivalence classes in C . The elements of the set:

$$[q] = \{\sqrt{\gamma(t)} O q(\gamma(t)) \mid O \in SO(3), \gamma \in \Gamma\} \quad (3)$$

are then deemed equivalent with the same shape. The resulting shape space is the set of of such equivalence classes:

$$S \doteq C / (SO(3) \times \Gamma) \quad (4)$$

To define geodesics on pre-shape and shape spaces we need a Riemannian metric. For this purpose we inherit the standard \mathbb{L}^2 metric the large space $\mathbb{L}^2(\mathbb{S}^1, \mathbb{R}^3)$. For any $u, v \in \mathbb{L}^2(\mathbb{S}^1, \mathbb{R}^3)$, the standard \mathbb{L}^2 inner-product is given by:

$$\langle\langle u, v \rangle\rangle = \int_{\mathbb{S}^1} \langle u(t), v(t) \rangle dt. \quad (5)$$

The computation of geodesics and geodesic distances utilize the intrinsic geometries of these spaces. While the detailed description of the geometries of C and S are given in [JKSJ07, SKJJ10].

Given two curves β^1 and β^2 , represented by their SRVF respectively q_1 and q_2 , we need to find a geodesic path between the orbits $[q_1]$ and $[q_2]$ in the space S . We use in this context, a numerical method called the path-straightening method [KS06] which connects the two points $[q_1]$ and $[q_2]$ an arbitrary path α and then updates this path repeatedly in the negative direction of the gradient of energy E .

It has been proven in [KS06] that the critical points of E are geodesic paths in S . We denote by $d(\beta^1, \beta^2)$ the geodesic distance between the corresponding equivalence classes $[q_1]$ and $[q_2]$ in S .

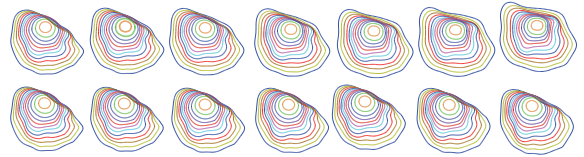


Figure 1: Examples of geodesic paths between two nasal surfaces. The first top row shows a geodesic path between nasal surfaces of two different persons, while the second bottom row is a geodesic path between nasal surfaces of two different sessions of the same person.

The Figure 1 illustrates two examples of geodesic paths between nasal curves.

3. 3D face authentication as a binary classification problem

We propose to use the well-known machine learning algorithm, AdaBoost, introduced by Freund and Schapire in [FS95], to learn a *strong classifier* based on a weighted selection of *weak classifiers*. In our case, the individual level curves are used to build the weak classifiers. The boosting can be then used to optimize their performances. AdaBoost

is based on iterative selection of weak classifiers by using a distribution of training samples. At each iteration, the classifier is provided and weighted by the quality of its classification.

3.1. Problem formulation

In authentication (called also verification) biometric scenario, the user provides both his/her biometric template and his/her identity to the system. Then, the task is to accept (a genuine user) or reject (an impostor) the claimed identity. A reliable authentication algorithm prohibits *impostors accesses* and authorizes *genuine accesses*. According to this definition, we can consider the authentication problem as a binary classification problem in which we define two classes, the impostor class I and genuine class G . Let us consider a curve β_λ^1 which belongs to a subject class C_p and β_λ^2 a curve which belongs to a subject class C_g and $d(\beta_\lambda^1, \beta_\lambda^2)$ denotes the distance between the curves β_λ^1 and β_λ^2 . Given a level curve λ , we define the classes I and G by:

- $I = \{d(\beta_\lambda^1, \beta_\lambda^2), \beta_\lambda^1 \in C_p, \beta_\lambda^2 \in C_g, i \neq j\}$.
- $G = \{d(\beta_\lambda^1, \beta_\lambda^2), \beta_\lambda^1 \in C_p, \beta_\lambda^2 \in C_g, i = j\}$.

Given overall distances between the curves of the each level λ , our goal is to build a binary classifier that minimizes the *False Accept Rate (FAR)* and the *False Reject Rate (FRR)*.

3.2. Adaboost for binary classification

The AdaBoost algorithm requires a training phase. This phase requires a set of training samples x_n including both I and G scores belonging to $X = \{x_n\}$. These samples are completely disjointed from the samples used for testing. To learn and then test AdaBoost algorithm, we use 2000 scans of 209 different subjects taken from FRGC v2 database [PFS*05]. We decompose this set into two subsets: the first one consists of 1052 scans/images for training and the second for the testing phase and contains 948 sessions. Then, we compute a similarity matrix for each phase for each level curve.

4. Experimental results

As described in Section 3, we use two subsets of the FRGC v2 database with one set to train the AdaBoost algorithm and a second to evaluate the classification results. We will use the evaluation rates used in conventional biometrics and particularly in the authentication scenario such as the (*Verification Rate*) VR , the (*False Accept Rate*) FAR , the (*False Reject Rate*) FRR , the (*True Reject Rate*) TRR . The similarity scores used are extracted randomly from the training matrix (or test) for the training phase (or test).

We give a comparison of Adaboost-based classifier results with the classification given by the sum rule d_{MA} , which is

the sum of all distances between the curves at the same level divided by the number of used curves. Here Λ is a finite set of values used in approximating a facial surface by facial curves. Assuming that $\{\beta_\lambda^1 | \lambda \in \Lambda\}$ and $\{\beta_\lambda^2 | \lambda \in \Lambda\}$ be the collections of facial curves associated with the two surfaces, d_{MA} is defined by:

$$d_{MA}(S^1, S^2) = \frac{1}{\lambda_0} \sum_{\lambda=1}^{\lambda_0} d(\beta_\lambda^1, \beta_\lambda^2) \quad (6)$$

We present results obtained in the testing phase. Having the final classifier, we present the testing samples. The classifier gives a binary decision (*genuine access/impostor access*). The results in table 1 shows the performance of our approach and shows the improvement of results compared to sum rule results.

| AdaBoost (Ad) and Sum rule (SR) | | | | | | | | |
|---------------------------------|--------------|--------------|------|----|--------------|--------------|-------|----|
| m, l | VR | | FAR | | FRR | | TRR | |
| | Ad | SR | Ad | SR | Ad | SR | Ad | SR |
| 2000 | 79.41 | 64.37 | 3.46 | | 20.59 | 35.63 | 96.54 | |
| 3000 | 79.87 | 69.79 | 4.61 | | 20.13 | 30.21 | 95.39 | |
| 4000 | 80.85 | 68.89 | 3.88 | | 19.16 | 31.11 | 96.13 | |
| 5000 | 81.50 | 68.18 | 3.04 | | 18.50 | 31.82 | 96.96 | |

Table 1: Results of authentication on the testing set, Ad: results given by using AdaBoost, SR: results given by the Sum rule

A more detailed analysis of this classifier shows that the classifiers associated to curves at $\lambda = 8$, $\lambda = 7$ and $\lambda = 3$ represent the more important weights in the Final classifier. The figure 2 shows the location of these curves on the nasal surface. These do not pass through the nostril and thus their shapes are not affected by these cavities presents in the nostrils. These cavities change the shapes of curves which affects the calculation of distances, in particular, the intra-class distances given by comparing two nasal surfaces of the same person.

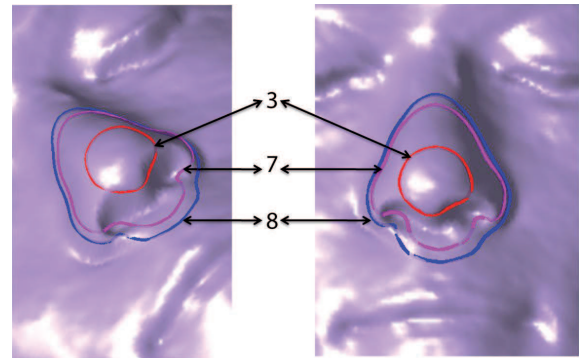


Figure 2: The location of the curves 8, 7 and 3 selected by AdaBoost

We calculated the pairwise distances between all curves, for different configurations of curves, for 2000 access genuines and access impostors. The Figure 3 shows four combinations : - (a) curves 3, 7 and 8, - (b) curves 1, 6 and 9 - (c) curves 2, 4 and 5 - (d) 3, 4 and 10. In Figure 3 a point represents a triple $\{d(c_3^i, c_3^j), d(c_7^i, c_7^j), d(c_8^i, c_8^j)\}$. We can observe that the sets of impostors access and genuines access are more separated in the case of similarity scores of curves 8, 3 and 7 compared to other combinations of curves. Therefore we can say that the AdaBoost algorithm has selected the best curves and gave them the strongest weight.

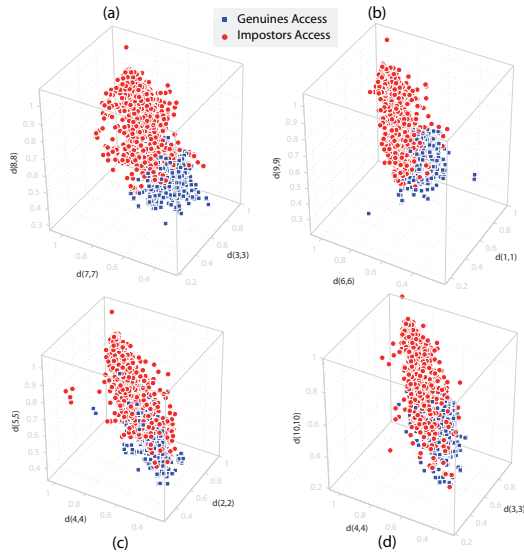


Figure 3: Different distributions of genuines access and impostors access for different combinations of curves: -(a) curves 3, 7 and 8 -(b) curves 1,6 and 9 -(c) curves 2, 4 and 5 -(d) 3, 4 and 10.)

5. Conclusion

In this paper we presented a new classifier based on the 3D curves for 3D nose authentication. We proposed using the AdaBoost algorithm to optimize the performance of authentication as a classification problem with binary decision. Based on a set of training set, AdaBoost select classifiers associated to the most relevant on the nose by attribute most important weights to their associated weak classifiers. Finally, we presented experiments on testing sets of varying sizes. These experiments show the interest of introducing the boosting to improve the authentication results. Future work will also concentrate on selecting 3D Curves on the facial surface from the whole FRGC v.2 database.

References

[AAC06] AMOR B. B., ARDABILIAN M., CHEN L.: New experiments on icp-based 3D face recognition and authentication. In

ICPR '06: Proceedings of the 18th International Conference on Pattern Recognition (2006), pp. 1195–1199.

[BBK07] BRONSTEIN A. M., BRONSTEIN M. M., KIMMEL R.: Expression-invariant representations of faces. *IEEE Transactions on Image Processing* 16, 1 (2007), 188–197.

[BV03] BLANZ V., VETTER T.: Face recognition based on fitting a 3D morphable model. *IEEE Transactions on Pattern Analysis and Machine Intelligence*. 25, 9 (2003), 1063–1074.

[CB07] CHEN H., BHANU B.: Human ear recognition in 3D. *IEEE Transactions on Pattern Analysis and Machine Intelligence* 29, 4 (2007), 718–737.

[CBF06] CHANG K. I., BOWYER K. W., FLYNN P. J.: Multiple nose region matching for 3D face recognition under varying facial expression. *IEEE Transactions on Pattern Analysis and Machine Intelligence* 28, 10 (2006), 1695–1700.

[DASD09] DRIRA H., AMOR B. B., SRIVASTAVA A., DAUDI M.: A riemannian analysis of 3D nose shapes for partial human biometrics. In *IEEE International Conference on Computer Vision* (2009), pp. 2050–2057.

[FBF08] FALTEMIER T., BOWYER K., FLYNN P.: A region ensemble for 3-d face recognition. *IEEE Transactions on Information Forensics and Security* 3, 1 (2008), 62–73.

[FS95] FREUND Y., SCHAPIRE R. E.: A decision-theoretic generalization of on-line learning and an application to boosting. In *EuroCOLT '95: Proceedings of the Second European Conference on Computational Learning Theory* (London, UK, 1995), Springer-Verlag, pp. 23–37.

[JKSJ07] JOSHI S. H., KLASSEN E., SRIVASTAVA A., JERMYN I. H.: A novel representation for efficient computation of geodesics between n -dimensional curves. In *IEEE CVPR* (2007), pp. 1–7.

[KS06] KLASSEN E., SRIVASTAVA A.: Geodesics between 3D closed curves using path-straightening. In *Proceedings of ECCV, Lecture Notes in Computer Science* (2006), pp. I: 95–106.

[KSMJ04] KLASSEN E., SRIVASTAVA A., MIO W., JOSHI S.: Analysis of planar shapes using geodesic paths on shape spaces. *IEEE Pattern Analysis and Machine Intelligence* 26, 3 (2004), 372–383.

[MMS07] MPIPEPIS I., MALASSIOTIS S., STRINTZIS M. G.: 3-d face recognition with the geodesic polar representation. *IEEE Transactions on Information Forensics and Security* 2, 3-2 (2007), 537–547.

[PFS*05] PHILLIPS P. J., FLYNN P. J., SCRUGGS W. T., BOWYER K. W., CHANG J., K. HOFFMAN, MARQUES J., MIN J., WOREK W. J.: Overview of the face recognition grand challenge. In *IEEE Computer Vision and Pattern Recognition* (2005), pp. 947–954.

[SKJJ10] SRIVASTAVA A., KLASSEN E., JOSHI S. H., JERMYN I. H.: Shape analysis of elastic curves in euclidean spaces. *IEEE Transactions on Pattern Analysis and Machine Intelligence accepted for publication* (2010).

[SSDK09] SAMIR C., SRIVASTAVA A., DAUDI M., KLASSEN E.: An intrinsic framework for analysis of facial surfaces. *International Journal of Computer Vision* 82, 1 (2009), 80–95.

[THV09] TER HAAR F. B., VELTKAMP R. C.: A 3D face matching framework for facial curves. vol. 71, pp. 77–91.

[YB07] YAN P., BOWYER K. W.: Biometric recognition using 3D ear shape. *IEEE Transactions on Pattern Analysis and Machine Intelligence* 29, 8 (2007), 1297–1308.

[You98] YOUNES L.: Computable elastic distance between shapes. *SIAM Journal of Applied Mathematics* 58 (1998), 565–586.